

## **3.5 CMSI projects**

# Nonadiabatic electron dynamics and many-body nuclear dynamics in molecules

Satoshi TAKAHASHI and Kazuo TAKATSUKA

*Department of Basic Science, Graduate School of Arts and Sciences, University of Tokyo  
Komaba, Meguro, Tokyo 153-8902*

To understand the quantum effects of nuclei in chemical reactions, it is necessary to track the wavepacket dynamics during the reactions. However, even with the modern massive parallel computers, it is still prohibitive to perform a primitive fully-quantum wavepacket dynamics simulations, because the required amount of calculation grows exponentially with the number of degrees of freedom. To overcome such a situation, we have been continuing researches based on the action decomposed function (ADF) [1, 2].

In the theoretical framework of ADF, wavepacket dynamics is described in terms of an ensemble of classical trajectories. Starting from the fundamental equation of ADF, it is found that dynamics is decomposed into two terms. One is proved to represent geometry of small spatial region around the reference trajectory, and the other is the “diffusion operator” with a pure imaginary diffusion constant.

Our preliminary numerical studies have already shown that the geometrical change around the reference path is described well with the nearby running ones, and also that quantum effects are able to be well incorporated thereby. These facts provide a significant advantage for the calculations of real systems with many degrees of freedom, because a reference trajectory, on which a volume element propagation is monitored, is reused as a nearby trajectory for some other nearby ones. Although we have not embarked on practical massive parallel computations based on this

theoretical formalism, we are going to make a start of many-body nuclear dynamics simulation, further proceeding to the connection to nonadiabatic electron dynamics.

Besides the advantage of describing multidimensional wavepacket dynamics, because of its structure, ADF theory also possesses an ability to reveal the quantum-classical correspondence in detail. Our previous study has made it clear that energy quantization is performed with action integrals and the so-called Maslov phases in the semiclassical regime [3]. However, such semiclassical phase quantization can yield a small deviation in the energy values, which becomes non-negligible when the Planck constant is large. Numerical tests based on the ADF has so far revealed the following facts: (i) It is the finiteness rather than being infinitesimal of the tiny volume element that allows to take the finite value of the Planck constant into account. (ii) Interference among propagated volume elements with initially different size also appears to be essential to reproduce quantum energy eigenvalues.

## References

- [1] S. Takahashi and K. Takatsuka: *Phys. Rev. A* **89** (2014) 012108.
- [2] K. Takatsuka and S. Takahashi: *Phys. Rev. A* **89** (2014) 012109.
- [3] S. Takahashi and K. Takatsuka: *J. Chem. Phys.* **127**, (2007) 084112.

# *Ab Initio* Calculation of High-Temperature Superconducting Mechanism – Comparison between Cuprates and Iron-Based Superconductors

Takahiro Misawa, Motoaki Hirayama, Takahiro Ohgoe, Terumasa Tadano,  
Youhei Yamaji, Kota Ido and Masatoshi Imada  
*Department of Applied Physics, University of Tokyo*  
*Hongo 7-3-1, Bunkyo-ku, Tokyo 113-8656*

A hierarchical method [1] (multi-scale *ab initio* scheme for strongly correlated electrons, MACE) developed by integration of the density functional theory (DFT) and the precise model calculation for strongly correlated electrons has been established a decade ago and is a promising way for treatments of electronic correlations beyond the standard DFT. In MACE, we first obtain the global band structures based on the DFT and evaluate the interaction parameters in the low-energy effective models by using constrained random-phase approximation following the idea of the renormalization group. Then, we solve the derived low-energy effective models by using precise low-energy solvers such as the many-variable variational Monte Carlo (mVMC) method. By using this scheme, we have successfully reproduced the electronic structures including the high- $T_c$  superconductivity of the iron-based superconductors [2].

However, in this scheme, there is a fundamental problem that the electronic correlations are doubly counted, i.e., the electronic correlations are included in both the DFT and the model calculations. Although this double counting is likely to be small in the MACE, in the strong coupling region where copper oxide high- $T_c$  superconductors are believed to be located, eliminating of the double counting offers

more reliable estimate for correctly reproducing the electronic structures.

In this project, to examine the effects of the double counting, we perform constrained *GW* (*cGW*) calculations [3]. In the *cGW* calculations, we first subtract the exchange-correlation energy in the LDA calculations and replace it with the *GW* self-energy that comes from only the high-energy degrees of freedom. In this procedure, since we do not consider the low-energy part of the *GW* self-energy in deriving the low-energy effective model, the double counting of exchange correlations does not occur. By performing *cGW* calculations for the cuprates, we find that the elimination of the double counting is quantitatively important to reproduce the realistic electronic structures of the cuprates.

Furthermore, in the cuprates, because the several bands entangle around the Fermi level, it is not clear what is the low-energy degrees of freedom. To identify the essential low-energy degrees of freedom, we have derived and solved single- and two-band models for two different cuprates ( $\text{HgBa}_2\text{CuO}_4$  and  $\text{La}_2\text{CuO}_4$ ). As a result, we find that the single-orbital ( $d_{x^2-y^2}$  orbital) model can be justified for  $\text{HgBa}_2\text{CuO}_4$ . In contrast to this, for  $\text{La}_2\text{CuO}_4$ , in addition to the  $d_{x^2-y^2}$  orbital, another orbital ( $d_{z^2}$  orbital) degrees of freedom play substantial roles. Our

detailed analysis on the low-energy effective models for the cuprates will provide a firm theoretical basis for understanding the origin of the high- $T_c$  superconductivity in the cuprates. The role of electron-phonon interactions can also be studied on unified grounds [4] and the detailed studies will be reported elsewhere.

### Acknowledgements

We thank Kosuke Miyatani for collaborations at the initial stage of this project and useful discussions.

### References

- [1] For a review, see M. Imada and T. Miyake, *J. Phys. Soc. Jpn.* **79**, 112001 (2010).
- [2] T. Misawa and M. Imada, *Nat. Commun* **5**, 5738 (2014).
- [3] M. Hirayama, T. Misawa, T. Miyake, and M. Imada, *J. Phys. Soc. Jpn.* **84**, 093703 (2015).
- [4] T. Ohgoe, and M. Imada, *Phys. Rev. B.* **89** 195139 (2014).

# DMRG Study of Kitaev-Heisenberg Model: from Honeycomb to Triangular Lattice

Takami TOHYAMA

*Department of Applied Physics, Tokyo University of Science, Tokyo 125-8585*

The Kitaev-Heisenberg (KH) model is suggested as an effective model for  $(\text{Na,Li})_2\text{IrO}_3$  that has a honeycomb lattice structure. The number of the bonds from each site on the honeycomb lattice is three. The same number appears on triangular lattice. Therefore, one can define a KH model on the triangular lattice. Furthermore, the triangular lattice is formed by putting a site at the center of the hexagonal unit of the honeycomb lattice. This leads to a motivation to study the models changing the interaction strength on the bonds connecting the central site and surrounding sites. It is also interesting how phases in the honeycomb lattices are connected to phases in the triangular lattice when the parameter values of the KH model are the same. For example, the honeycomb Kitaev model show a spin-liquid phase, while the triangular Kitaev model gives a nematic phase. The change of the two phases is an interesting issue to be studied theoretically. We note that our group has already studied the KH model on both lattices [1, 2].

We examine the KH model by changing the interaction connecting the both lattices by the two-dimensional density-matrix renormalization group (2D-DMRG) method for a  $12 \times 6$ -site lattice. We used the System C in the Supercomputer Center, the Institute for Solid State Physics, the University of Tokyo, and the K-computer. The 2D-DMRG code has been developed by our group. To perform DMRG, we map the original system to a snake-like one-dimensional chain, and combine the chain with long-range interactions. We keep nearly

1000 states in the DMRG block and performed nearly 10 sweeps, resulting in a typical truncation error with the order of  $10^{-5}$ . Calculating the ground-state energy, spin structure factors, and entanglement properties, we preliminarily obtain the ground state phase diagram of the Kitaev-Heisenberg model as a function of the strength of the connecting interaction.

We focus on the Kitaev model without the Heisenberg terms, since the end points exhibit interesting phases: a nematic phase and a spin-liquid phase for the triangular and honeycomb lattice, respectively. Since the Kitaev spin-liquid phase is weak against additional interaction, it is destroyed as soon as the connecting interaction is turned on. The same is for the other end where the nematic phase exists. These weakness means the presence of another phase between the honeycomb and triangular Kitaev models, which is a stripy phase. A detailed examination is now in progress together with the construction of the detailed phase diagram with full parameter region.

This work was done in collaboration with Shigetoshi Sota.

## References

- [1] K. Shinjo, S. Sota, and T. Tohyama: Phys. Rev. B **91** 054401 (2015).
- [2] K. Shinjo, S. Sota, S. Yunoki, K. Totsuka, and T. Tohyama: arXiv:1512.02334.

# Study of Novel Quantum Phases and Critical Phenomena by Monte Carlo Method and Tensor Network --- SU( $N$ ) Heisenberg Model with Multicolumn Representations

Tsuyoshi Okubo<sup>1</sup>, Kenji Harada<sup>2</sup>, Jie Lou<sup>3</sup>, and Naoki KAWASHIMA<sup>1</sup>

<sup>1</sup>*Institute for Solid State Physics, The University of Tokyo, Kashiwa-no-ha, Kashiwa, Chiba 277-8581,*

<sup>2</sup>*Graduate School of Informatics, Kyoto University, Kyoto 606-8501, Japan,*

<sup>3</sup>*Department of Physics, Fudan University, Shanghai 200433, China*

Quantum spin liquid states and topological states are among the most intensively investigated subjects in the recent condensed matter theory. In our project, we consider several quantum spin systems as characteristic examples for studying these novel states and related quantum phase transitions. We also develop computer programs specialized for large scale parallelization aiming at the K-computer. In particular, we investigate the SU( $N$ )  $J$ - $Q$  model, to clarify the nature of the deconfined critical phenomena. In general, our model is the Heisenberg generalized in two ways: the spin operators are generators of SU( $N$ ) ( $N=2,3,4,\dots$ ) algebra instead of the conventional SU(2) spins, and the model has 4 or 6-spin interactions in addition to the conventional 2-spin nearest neighbor interactions.

However, in the present report, we concentrate on the effect of representations and only discuss the case with no multi-spin interactions. To be specific, our Hamiltonian is

$$H = \frac{J}{N} \sum_{\langle ij \rangle} \sum_{\alpha, \beta=1}^N S_i^{\alpha\beta} \bar{S}_j^{\beta\alpha},$$

where  $i$  runs over lattice points of one of the two sublattices of square lattice. The symbol  $S_i^{\alpha\beta}$  represent an SU( $N$ ) spin in  $n$ -column and single-row representation whereas  $\bar{S}_i^{\beta\alpha}$  in the conjugate representation, i.e.,  $n$ -column and  $(N-1)$ -row representation.

We used an original code developed based on the ALPS/Looper, a program package based on the loop algorithm of the world-line

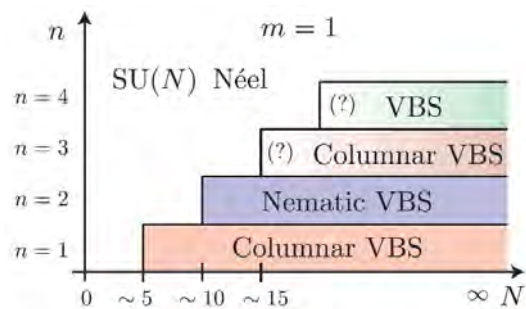


Fig. 1 Schematic phase diagram of the SU( $N$ ) Heisenberg model on the square lattice with single-row representations. (Adapted from Ref.[1].)

quantum Monte Carlo simulation.

In this report, the central question is whether the intermediate spin-liquid state exist or not in the  $n$ - $N$  phase diagram of the generalized Heisenberg model. For  $n=1$  (fundamental representation), it had been established [2] that the transition occurs from the magnetic state (Néel state) for  $N \leq 4$  to the non-magnetic state for  $N \geq 5$ , where the latter non-magnetic phase is the valence bond solid (VBS) state with spontaneously broken lattice-rotational symmetry.

We carried out calculation for  $n=2$  and 3 for  $N \leq 25$ . The system size studied was  $L = J/T \leq 128$ . From our calculation, we found no evidence for the intermediate spin liquid state. To be more specific, for  $n=2$ , we found that the ground state is the Néel state for  $N \leq 9$  and the

VBS state for  $N \geq 10$ . For  $n=3$ , we found that the ground state is the Néel state for  $N \leq 14$  and that the magnetic order is absent for  $N \geq 15$ . Unlike the case of  $n=2$ , we could not detect any other order for  $N \geq 15$ . However, we do not take this observation as an evidence for the intermediate spin-liquid state because our estimate of the amplitude of the VBS order parameter based on the field theory suggests that it could well be too small for the present precision to detect.

## References

- [1] Tsuyoshi Okubo, Kenji Harada, Jie Lou, Naoki Kawashima, Phys. Rev. B **92** (2015) 134404(1-5).
- [2] N. Kawashima and Y. Tanabe, Phys. Rev. Lett. **98**, (2007) 057202



## Multi-scale simulation of nano-structured devices from electronic structures to mechanical properties

Shuji OGATA

*Nagoya Institute of Technology*

*Gokiso-cho, Showa-ku, Nagoya 466-8555, Japan*

In the fiscal year of 2015, we have mainly treated three subjects. The first one is the hybrid quantum-classical (QM-CL) simulation study of the thermal diffusion of correlated Li-ions in graphite. The second one is the classical molecular-dynamics (MD) simulation study of the heat transfer through alumina/epoxy/alumina system. The third one is the hybrid QM-CL simulation study of Si-O bond breaking in silica glass. Those are described briefly as follows.

*Subject 1: The hybrid QM-CL simulation of the thermal diffusion of Li-ions in graphite [1].* Diffusion of Li-ions in graphite is an essential elementary process in the current lithium-ion battery. The C-layers of graphite deform with Li due to relatively large size of Li-ion, which acts to confine the Li-ions and thereby create correlation between them. We address theoretically the thermal diffusivity of such correlated Li-ions in graphite by the hybrid quantum-classical simulation method. In this method, the quantum-region composed of the Li-ions and surrounding C atoms is treated by the density-functional theory, while it is embedded dynamically in the total system described with an empirical inter-atomic interaction potential. We thereby take into account the long-ranged deformation field in graphite in simulating the Li-ion dynamics.

We perform the hybrid simulation run with 14 Li-ions inserted, 7 by 7, to two inter-layer spaces of graphite (ten C-layers). The stacking structures of the C-layers that sandwich Li-ions are the AA-stacking. The largest QM-region contains 625 C-atoms and 11 Li-ions; it takes about 9 minutes per time step using about 100 CPU's of Fujitsu FX10 at ISSP with the domain decomposition  $2 \times 2 \times 1$ , the spatial decomposition of each domain  $5 \times 5 \times$

3, the band parallelization 2, and the OpenMP parallelization 4 set in the divide-and-conquer-type  $O(N)$ -RGDFT (named DC-RGDFT) code.

*Subject 2: The MD simulation of the heat transfer through alumina/epoxy/alumina system [2].* The composite of epoxy polymers and  $\alpha$ -alumina fillers is used as a heat dissipation material. The fillers often agglomerate with nanometer-depth polymers sandwiched in between. We address theoretically the effective thermal conductivity of such a filler-polymer-filler system (see Fig. 1). The non-equilibrium MD simulation is performed to obtain the effective thermal conductivity of the system, in which bisphenol-A (bisA) epoxy polymer sub-system with depth 14–70 Å is inserted between two  $\alpha$ -alumina slabs. Effects of surface-coupling (SC) agent are also investigated by adding model molecules to the

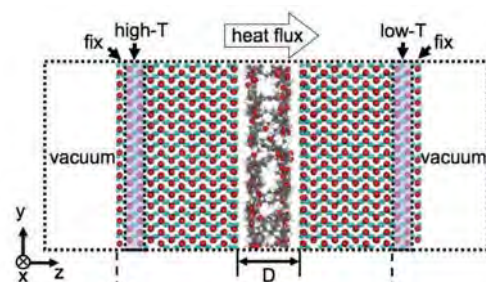


Figure 1: Atomic configuration of a typical system for the NEMD simulation with  $D = 14$  Å without the SC molecules. Large red spheres are O's; medium cyan, Al's; medium grey, C's; small white, H's.

polymer sub-system.

For smaller polymer-depth cases, the effective thermal conductivity is determined essentially by the interfacial thermal



conductance that relates to the temperature-gaps at the interfaces. We find for the interfacial thermal conductance that: (i) it is decreased by decreasing the polymer depth toward the chain length of a single bisA molecule, and (ii) it is increased by adding the SC molecules to the polymer sub-system. Combining separate simulation analyses, we show that the (i) results from effectively weakened interaction between a bisA molecule and two  $\alpha$ -alumina slabs due to the orientation constraint on the bisA molecule by the slabs. Reasons of the (ii) are enhancement of the following three quantities by addition of the SC molecules: the phonon population of the bisA molecules at those frequencies corresponding to that of acoustic phonons of  $\alpha$ -alumina, the phonon transmission coefficient from the  $\alpha$ -alumina slab to the polymer sub-system for the transverse acoustic phonon, and the group velocity of the transverse acoustic phonon in the polymer sub-system.

*Subject 3: The hybrid QM-CL simulation of Si-O bond breaking in silica glass [3].* We perform a hybrid QM-CL simulation of a 4,608-atom silica glass at a temperature of 400 K with either a water monomer or dimer inserted in a void (see Fig. 2). The quantum region that includes the water and the surrounding atoms is treated by the DFT. During a simulation, the silica glass is gradually compressed or expanded. No Si-O bond breaking occurs with a water monomer until the silica glass collapses. With a water dimer, we find that Si-O bond breaking occurs through three steps in 3 out of 24 compression cases: (i) H-transfer as  $2\text{H}_2\text{O} \rightarrow \text{OH}^- + \text{H}_3\text{O}^+$  accompanied by the adsorption of  $\text{OH}^-$  at a strained Si to make it five-coordinated, (ii) breaking of a Si-O bond that originates from the five-coordinated Si, and (iii) H-transfer from  $\text{H}_3\text{O}^+$  to the O of the broken Si-O bond. A separate DFT calculation confirms that the barrier energy of the bond breaking with a water dimer under compression is smaller than that with a water monomer and that the barrier energy decreases significantly when the silica glass is compressed further.

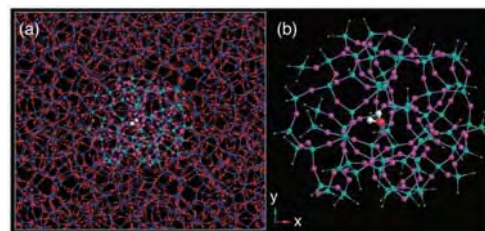


Figure 2: (a) Present silica glass with a water molecule in a void. The red and blue spheres are CL O and Si, respectively. The magenta and cyan spheres are QM O and Si, respectively. The large red and white spheres are respectively QM O and H of a water molecule. (b) Atomic cluster used for the QM calculation.

## References

- [1] N. Ohba, S. Ogata, T. Kouno, and R. Asahi, *Comp. Mater. Sci.* **108** (2015) 250-257.
- [2] K. Tanaka, S. Ogata, R. Kobayashi, T. Tamura, and T. Kouno, *Int. J. Heat and Mass Transfer* **89** (2015) 714-723.
- [3] T. Kouno, S. Ogata, T. Shimada, T. Tamura, and R. Kobayashi, *J. Phys. Soc. Jpn.* **85** (2016), in press.

# Highly accurate calculation of impurity hydrogen in oxides

Shinji TSUNEYUKI

*Department of Physics, School of Science, The University of Tokyo*

*7-3-1 Hongo, Bunkyo-ku, Tokyo 113-0033*

*Institute for Solid State Physics, The University of Tokyo*

*Kashiwa-no-ha, Kashiwa, Chiba 277-8581*

Impurity hydrogen is known to play a crucial role for electronic properties of semiconductors. It does not only terminate dangling bonds of defects or surface of semiconductors but also passivate carriers in both p-type and n-type semiconductors by changing its charge state to a cation ( $H^+$ ) or an anion ( $H^-$ ), respectively. Impurity hydrogen is also attracting much attention as a carrier dopant in oxide semiconductors and superconductors.

Direct observation of the existence and charge state of impurity hydrogen is so difficult that there have been a lot of theoretical studies with the first-principles calculation based on the density functional theory (DFT). However, the accuracy of the total energy calculated by DFT is considered to be insufficient for conclusive prediction of the stable charge state of impurity hydrogen. In this project, we used the diffusion Monte Carlo method, a state-of-the-art first-principles total-energy calculation method, to clarify the most stable charge state of impurity hydrogen in crystalline  $SiO_2$ ,

Neutral  $H^0$  does not exist in  $SiO_2$  by ESR study except when the sample is irradiated by an electron beam, meaning that  $H^0$  is not a stable state of impurity hydrogen. On the other hand, in  $\mu SR$  study, it is known that a large portion of muon impinged in low-quartz, a typical polymorph of  $SiO_2$ , turns into a muonium (Mu), a bound state of a muon and an electron. It suggests the stability of  $H^0$ . Mu is also ob-

served in stishovite, a high-pressure polymorph of  $SiO_2$ . From the DFT calculation of low-quartz and stishovite, a typical polymorph of  $SiO_2$ , the stable charge state of impurity hydrogen is either  $H^+$  or  $H^-$  depending on the electron chemical potential and  $H^0$  is unstable in any condition. Here we calculated the total energy of impurity hydrogen in low-quartz and stishovite changing its position and charge states by DMC to find that the DFT results are qualitatively reproduced, that is,  $H^0$  is energetically unstable in thermal equilibrium.

From the present calculation we conclude that the Mu observed in  $\mu SR$  experiments are realized only as a metastable state. To confirm the metastability of Mu (or  $H^0$ ), we developed a method to find activation barrier for the diffusion of an impurity considering the change in its charge state. The method is based on the nudged elastic band (NEB) method but potential energy hypersurfaces for different charge states are considered. With the method, we investigated the stability of hydrogen impurity ( $H^0$ ,  $H^+$ ,  $H^-$ ) in  $SiO_2$  to find the neutral state can be actually realized by large activation energy barriers [1].

## References

- [1] Y. Yamamoto, R. Akashi and S. Tsuneyuki, in preparation.

## Materials design for spintronics/multiferroics applications

Mineo SAITO, Tasuki, ODA and Fumiyuki ISHII

*Division of Mathematical and Physical Science, Institute of Science and Technology,  
Kanazawa University, Kakuma, Kanazawa, 920-1192 Japan*

In this project, we have developed codes which enable the study of spintronics and multiferroics materials. We have developed a program code of newly parallelized density functional electronic structure calculations (CPVO). We also make a program that enables drawing spin textures by using numerical results which are calculated by using the OpenMX code.

We have performed the first-principles density functional calculation for the slab systems; single interface MgO/Fe, magnetic junction Fe/MgO/Fe, the double interface MgO/Fe/MgO, and Fe/TiO<sub>2</sub>/SrO/TiO<sub>2</sub> [1]. To clarify the origin of electric field (EF) effect on the magnetic anisotropy energy (MAE), we discussed the electronic structure of interface Fe with using the calculated results. In these studies, we found that the EF-induced modulation sign of MAE is reversed when the dielectric material is changed to SrTiO<sub>2</sub>(STO) from MgO. In the STO systems, the MAE decreases as the electron depletion condition (positive EF) is induced in the interface using the external EF. However, as shown in Fig. 1, the number of electrons (NOE) slightly increases as the EF, associated with the

decrease of spin magnetic moment (SM) on the interface Fe. This decrease of SM is consistent with an increase of NOE assuming a usual simple exchange-splitting band model. In Fig. 1, however, the increasing ratio on NOE is not so high (rather small), compared with the absolute of decreasing ratio on SM. This situation may be understood by considering that under the EF the 3d electron increases and other 4s electron decreases on the interface Fe. When assuming the decrease of 3d electron, the decrease of MAE may be explained by the general property in the Fe thin film, so that the MAE decreases as number of electrons.

The partial density of states projected to the Fe atom at interface was calculated Fe/TiO<sub>2</sub>/SrO/TiO<sub>2</sub>, for shown in Fig. 2. In these PDOSs, the minority spin states of 3d orbitals are located around the Fermi level ( $E_F$ ). When compared with the corresponding quantities of Fe/MgO systems, the Fermi level is located at the lower energy. This energy is far from the interface resonance states (IRS) which are observed as spiky peaks just above the Fermi level in the PDOS. Although such property may be one of the circumstantial evidences which deduce the decreasing behavior in MAE with

respect to EF, no adequate mechanism has been proposed yet. Further investigations are required.

We have been studying ZnO and found the possibility of its application to spintronics devices [2-3]. In this study [4], we find that metallic spin-split surface bands can be achieved on hydrogenated ZnO (10-10) surface (Fig. 3). We clarify that the hydrogenation plays an important role in spin-orbit interaction and the spin-split bands induce strongly anisotropic Rashba-type spin textures, which are expected to be useful for device applications.

### References

- [1] D. Yoshikawa et al., ICM2015, Barcelona (Spain), July 2015.
- [2] M. A. U. Absor et al, Appl. Phys. Express 7, 053002 (2014).
- [3] M. A. U. Absor et al, Appl. Phys. Express 8, 073006 (2015).
- [4] M. A. U. Absor et al, AIP Advances 6, 025309 (2016).

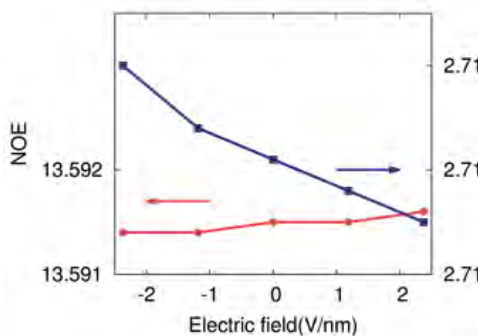


Fig 1. Number of electron (NOE) and spin magnetic moment as a function of electric field.

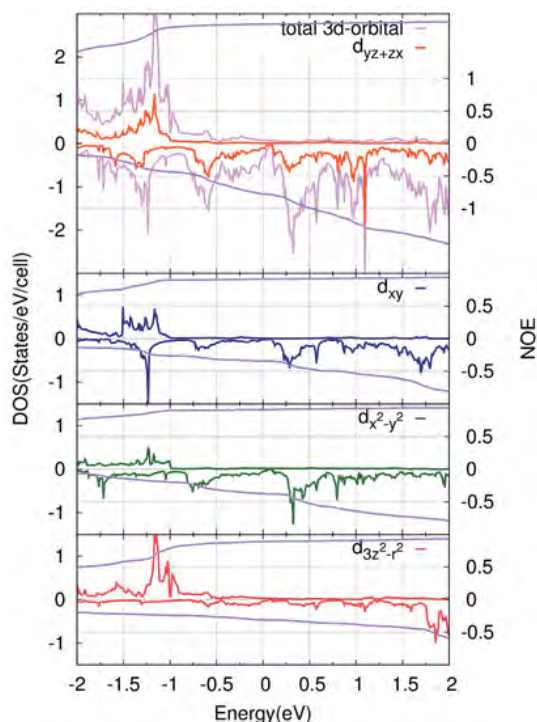


Fig 2. Partial density of states (PDOS) on the Fe atom at the interface Fe/TiO<sub>2</sub>/SrO/TiO<sub>2</sub>.

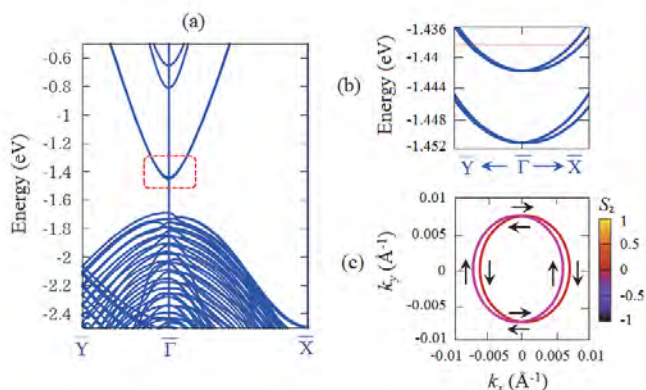


Fig 3. Electronic band structure (a), (b) and spin-resolved isoenergy line at -1.4eV (c) of hydrogen terminated ZnO (10-10).

## Photo-induced electron dynamics in nanostructures and development of quantum devices with optical and electronic functionality

Katsuyuki NOBUSADA

*Institute for Molecular Science,*

*Myodaiji, Okazaki, Aichi 444-8585*

An optical near-field (ONF) is a nonpropagating light localized in proximity to a surface or, more precisely, an interface region between materials, such as nanoparticles in the air, dopants or holes embedded in solids, and interfaces between different dielectrics. ONFs have been discussed very frequently in the context of electric field enhancement in nanometer regions far beyond the diffraction limit. The field enhancement due to plasmon excitation in metals such as precious metal clusters is a major topic in the field of plasmonics. However, a more intrinsic feature of ONFs, which causes qualitatively different electron excitation from that of a far-field light, is the nonuniformity of the electric field [1]. Since an ONF rapidly decays with increasing distance from ONF source, the electric field gradient plays an important role in the ONF and matter interaction. In such an interaction, matter experiences a nonuniform electric field that is qualitatively different from the uniform far-field propagating light. Thus, the conventional theoretical treatment of a light-matter interaction based on a dipole

approximation does not work well.

We have illustrated an unusual dynamical interaction effect between an ONF and electrons. This dynamical ONF effect was introduced in our studies [1], in which we showed that the ONF excitation inherently includes a second-harmonic electric field component, derived from the dynamical interaction between the ONF and the electron. As an example, we demonstrated the ONF induced two-photon absorption in a real nanostructure of a metal-organic-framework (MOF). More specifically, an acetylene molecule is efficiently two-photon excited by the ONF generated in the MOF. The MOF is highly ordered and large nanostructures. Our originally developed computational program called GCEED [2] allows us to perform massively parallelized calculations of such ONF excitation dynamics in the MOF.

We also started first-principles molecular dynamics simulations of metal cluster catalysts supported on solid surfaces. Catalytic CO oxidation on a gold or platinum supported cluster has proved to occur through Langmuir-

Hinshelwood mechanism [3,4].

### References

- [1] M. Yamaguchi, K. Nobusada and T. Yatsui, *Phys. Rev. A*, **92**, 043809 (2015).  
[2] M. Noda, K. Ishimura, K. Nobusada, K.

Yabana and T. Boku, *J. Comp. Phys.*, **265**, 145 (2014).

- [3] K. Koizumi, K. Nobusada and M. Boero, *Chem. Eur. J.* **22**, 5181 (2016).  
[4] K. Koizumi, K. Nobusada and M. Boero, *J. Phys. Chem. C* **119**, 15421 (2015).



# Molecular Science of Virus by All-Atom Simulation

Susumu Okazaki

*Department of Applied Chemistry, Nagoya University  
Furo-cho, Chikusa-ku, Nagoya, 444-0868*

In fiscal 2015, our group used the system-B in the second half year and the system-C throughout the year. We carried out the molecular dynamics (MD) calculation with respect to the stability of poliovirus empty capsids in electrolyte solution[1] and the interaction between poliovirus capsids and its receptor CD155. These systems contain  $10^6 - 10^7$  charged atoms. Electrostatic interactions among the charges were calculated under the three dimensional periodic boundary condition based on the fast multipole method. Further, the machine time was used to analyze trajectories of production runs of poliovirus systems generated on the K computer.

Analyses were carried out using parallelized programs by MPI and OpenMP, and partially OpenACC, combined with MODYLAS[2]. Interactions between the capsid and D1 domain of CD155 was evaluated calculating the free energy profile as a function of radial distance between the two. The attractive forces do act between the capsid and receptor. Further, analysis on the electric field around poliovirus capsids was conducted, which provided valuable information to understand the origin of a specific interaction between poliovirus capsid and CD155-D1. MD calculation studies on physical properties of lipid bilayers modeling hepatocyte plasma membranes[3] were carried out, too. This contributes to understanding of the

physico-chemical properties of the envelope of Hepatitis B viruses.

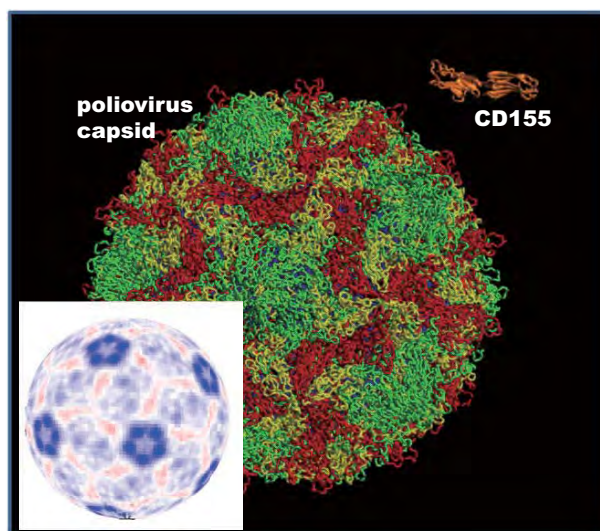


Figure 1: Poliovirus capsid and poliovirus receptor CD155. Ions and waters are not shown. Inserted figure is an example of the calculated electric field around the capsid.

## References

- [1] Y. Andoh, et al. : J. Chem. Phys., **141** (2014) 165101.
- [2] Y. Andoh, et al. : J. Chem. Theory Comput. **9** (2013) 3201.
- [3] Y. Andoh, et al. : J. Chem. Phys., **144** (2016) 085104.



# Large scale ab initio calculations on the fundamental processes of energy convergence devices and on their optimization for high conversion efficiency

Koichi YAMASHITA

Department of Chemical System Engineering,

*The University of Tokyo, Hongo, Bunkyo-ku, Tokyo 113-8656*

Organic photovoltaic (OPV) cells are being eagerly researched and developed. In particular, bulk heterojunction (BHJ) photovoltaic cells have many attractive properties. Exciton dissociation that leads to generation of free electron and hole has been considered as a key factor in photo-conversion process of OPVs. However, the fine mechanism of the exciton dissociation against Coulomb interaction between the electrons and holes has not been fully revealed yet. Then, we studied (1) charge recombination which depress the power conversion efficiency of OPVs [1] and (2) short-circuit currents which is determined by competition of the charge dissociation and charge recombination [2, 3]. In both studies, we used our original code named as MolDS that is implemented for massive parallel computing of semiempirical quantum calculations, especially electronic excited states calculations, by using hybrid (openMP/MPI) parallelization technique. In the first part, the electronic structures of P3HT at the interface and in the bulk phase were investigated to elucidate the charge

separation process in the P3HT/SWNT blends. We found energy difference between the HOMO levels at the interface and those in the bulk phase, which explains observations in a previous experiment where long-lived charge carriers were only observed in blends containing excess P3HT. In the second part, we found that a pair of donor and acceptor exhibits the largest charge-bridging upon photo-absorption, which leads to the highest IQE and PCE. This later finding should be a unique guiding principle to synthesize new molecular materials for OPVs.

## References

- [1] K. Nishimra, M. Fujii, R. Jono, and K. Yamashita: *J. Phys. Chem. C* **119**, 26258-26265 (2015)
- [2] M. Fujii, W. Shin, T. Yasuda, and K. Yamashita: *Phys Chem Chem Phys.* **18**, 9514-9523, (2016)
- [3] S. Koda, M. Fujii, S. Hatamiya, K. Yamashita: *Theor. Chem. Acc.* **135**, 115-124, (2016)
- [4] M. Fujii, K. Nishimra, M. Okuyama, MolDS  
URL: <https://en.osdn.jp/projects/molds/>

## Surface/Interface Science of Energy Conversion

Osamu SUGINO

*Institute for Solid State Physics, University of Tokyo  
Kashiwa-no-ha, Kashiwa, Chiba 277-8581*

This article reports work done by members of the priority project of CMSI[1], aiming at establishing a first-principles approach to the electrochemical interface. The target consists of the two; the electrocatalyst-solution interface typical of the fuel-cell study and the solid-electrolyte interface typical of the battery study. The former study is mainly based on the package called STATE which has been developed by Morikawa group, and the latter is based on stat-CPMD developed by Tateyama group. Both codes have been specialized to the interface study and are able to obtain equilibrium structures of the interface and free-energy of the electrochemical reactions: The codes are parallelized not only w.r.t. the typical parallelization axes[2] but also w.r.t. the reaction coordinates, by which the free-energy landscape can be obtained by a single run. Major problem encountered therein is that the reaction coordinate needs to be assumed before the simulation but the reaction does not always proceed as assumed[3], reflecting a number of competing reaction sites appearing in the simulation cell. This means the method developed in quantum chemistry cannot be applied to the complex interface, requiring us to develop a distinct one. In this context, we have focused on a method developed by Morishita[4], which allows us to correct the reaction coordinate on the fly, and implemented the method to STATE. Our test calculation shows a promise in applying to realistic electrocatalytic reactions to predict a current voltage curve from first-principles.

In the study of battery, the relevant process

is often the bias-induced shift of equilibrium between the solid and the electrolyte, where the simulation is demanding compared with that for the electrocatalytic reaction. The required spatial and time scales exceed achievable by the first-principles simulation. In this context, we have developed a procedure to construct a force field model on the basis of first-principles calculation using a modern statistical technique with which to perform a larger-scale (ten thousands of molecules and sub-micro second long) simulation. The simulation on  $2\text{Li} + \text{O}_2 \rightleftharpoons \text{Li}_2\text{O}_2$  revealed that the oxide nucleates differently in the ionic liquid (EMI-TFSI) and in the organic solvent (DMSO) when discharging, and that the oxide dissolves only partially and remains as  $\text{Li}_3\text{O}_2^+$  when charging [5]. The experimental study is still difficult for this lithium-air battery system, and our theoretical prediction is expected to provide particularly useful information.

Group IV oxides, such as  $\text{Ta}_2\text{O}_5$  or  $\text{ZrO}_2$ , are regarded as a next-generation fuel-cell electrocatalyst because of its better durability than that of Pt. The oxide catalysts have long been the target of electrochemistry but the microscopic process is still unknown. In this context, we started the study of a monoclinic  $\text{ZrO}_2$  surface by investigating if the pristine surface would be active enough or needs modification to be reactive. We have investigated how the activity can be improved by introducing oxygen vacancies together with nitrogen impurities, as suggested by experimentalists. We have not yet successful in explaining the experimentally observed activity and thus there

will be a room for improving the modeling.

## References

- [1] The project members are Y. Morikawa (Osaka University), K. Inagaki (Osaka University), H. Kizaki (Osaka University), Y. Tateyama (NIMS), K. Sodeyama (NIMS), K. Akagi (Tohoku University), M. Otani (AIST), O. Sugino (ISSP) and S. Kasamatsu (ISSP).
- [2] The band axis, the G-point axis, and the k-point axis. Through parallelization w.r.t. these axes, we have achieved good parallel efficiency at least up to a few thousand of atoms. The average CPU usage is  $\sim 20\%$ .
- [3] I. Hamada and O. Sugino, *Hyomen Kagaku* **34**, 638 (2013).
- [4] T. Morishita, S. G. Ito, H. Okumura and M. Mikami, *J. Compt. Chem.* **34**, 1375 (2013). The method developed herein is based on logarithmic mean force dynamics (log-MFD); Morishita et al., *Phys. Rev.* **E 85**, 066702 (2012).
- [5] K. Akagi et al. (submitted)

# Role of calcium ion in molecular recognition process of calcium-dependent carbohydrate-binding module

Norio YOSHIDA

*Department of Chemistry, Graduate School of Science*

*Kyushu University, 744 Motoooka, Nishi-ku, Fukuoka 809-0395*

The enzymatic degradation of polysaccharides is an important process in the cell wall biomass creation. The carbohydrate-active enzymes have a module to recognize the carbohydrate chain, called carbohydrate-binding module (CBM). The carbohydrate binding by a CBM is the initial process of carbohydrate degradation and also the rate-determining process of the reaction. CBMs are classified into numerous families, and each family has different mechanism of the selective recognition of carbohydrates. Xylanase 43 from *Paenibacillus polymyxa* is a three-module protein that has Ca<sup>2+</sup>-dependent xylan binding module (CBM36).[1]

The mechanism of xylan binding of CBM36 and the role of Ca<sup>2+</sup> ion were investigated by the combinational use of the molecular dynamics (MD) simulation and the three-dimensional reference interaction site model (3D-RISM) method.[2]

The Ca<sup>2+</sup>-bound CBM36 showed xylan affinity, while the Mg<sup>2+</sup>-bound CBM36 showed no affinity. The free energy component analysis for the xylan binding

process revealed that the major factor of the xylan affinity is the electrostatic interaction between the Ca<sup>2+</sup> ion and the hydroxyl oxygens of xylan. The van der Waals interaction between the hydrophobic side chain and the xylan also contributes to the stabilization. The dehydration by the complex formation has the opposite effect on those interactions. In the case of the Ca<sup>2+</sup>-bound CBM these interactions are well balanced, while in the case of the Mg<sup>2+</sup>-bound CBM the dehydration penalty is too large.

The details of the xylan binding of CBM36 are revealed at the molecular level by this study. It is expected that the results of this study contribute to the design of highly efficient CBM or the control of the selectivity of polysaccharides.

## References

- [1] S. Jamal-Talabani, A.B. Boraston, J.P. Turkenburg, N. Tarbouriech, V.M. Ducros, G.J. Davies, *Structure* 12 (2004) 1177.
- [2] S. Tanimoto, M. Higashi, N. Yoshida, H. Nakano, Submitted.

# First Principles Calculation of Properties of MXene Electrode Materials under Bias

Minoru OTANI<sup>1,2</sup>, Chunping HU<sup>1,2</sup>

<sup>1</sup>*Research Center for Computational Design of Advanced Functional Materials (CD-FMat), National Institute of Advanced Industrial Science and Technology (AIST), Tsukuba, Ibaraki, 305-8565, Japan*

<sup>2</sup>*Elements Strategy Initiative for Catalysts and Batteries (ESICB), Kyoto University, 1-30 Goryo-Ohara, Nishikyo-ku, Kyoto 615-8245, Japan*

Sodium ion batteries (SIBs) have been rapidly developed since 2010, on the basis of research and development of lithium ion batteries (LIBs) [1]. In order to improve the battery performance, it is an urgent task to develop new hardly-degraded electrode materials for SIBs, as Na intercalation/extraction process would incur much larger volume expansion/shrinkage if using existing electrode materials for LIBs. Very recently a new type of negative electrode materials – MXene – has been developed for SIBs and found to be very stable during the charging-discharging cycles in which the inter-layer distance of MXene can be kept constant [2]. Great interests have been aroused for the theoretical investigation of properties of MXene, however, first principles study considering the effect of bias voltages has not been carried out yet.

In the present work, we use the effective screening medium (ESM) method developed by Otani and Sugino [3] to study the effect of bias voltages on the properties of MXene with or without ion adsorption, within the planewave pseudopotential framework of density functional theory. The *ab initio* program package QUANTUM ESPRESSO [4] was used and numerical calculations were done in System B and C. In order to achieve the experimental condition of constant bias voltages, the chemical potential of electrons in the electrode

is kept constant by adjusting the charge of the system [5].

First, we carried out extensive studies on the surface termination of MXene under bias using mono-, bi- and tri-layer models either terminated by F, O, or OH atoms. All these atoms are found to be bonded to Ti<sub>2</sub>C on the Ti site with or without bias voltages. Next, as a comparative study, we calculated Li adsorption and diffusion on a (3×3) supercell of monolayer Ti<sub>2</sub>CO<sub>2</sub>. Upon a bias of ±2 V, the Li adsorption sites do not change, but the Li diffusion barrier was found to be varied by more than 50 meV. This shows that although the bias voltage has little effect on ion adsorption, it significantly affect ion diffusion on MXene.

## References

- [1] K. Kubota and S. Komaba, *J. Electrochem. Soc.* **162**, A2538 (2015).
- [2] X. Wang *et al.*, *Nat. Commun.* **6**, 6544 (2015).
- [3] M. Otani and O. Sugino, *Phys. Rev. B* **73**, 115407 (2006).
- [4] P. Giannozzi *et al.*, *J. Phys.: Condens. Matter* **21**, 395502 (2009).
- [5] C. Hu and M. Otani, to be submitted to *Phys. Rev. Lett.*

# All electron spectra and dynamics of functional materials from nanoclusters to crystals

Kaoru Ohno

*Department of Physics, Faculty of Engineering Science,*

*Yokohama National University, Tokiwadai, Hodogaya-ku, Yokohama 240-8501*

To obtain all-electron spectra and dynamics of functional materials from nanoclusters to crystals, a versatile program TOMBO Ver.2 is developed using the all-electron mixed basis approach, which removes weak points of the preexisting first-principles methods. Ground- and excited-state chemical reactions can be treated within the DFT, TDDFT, and TDGW formalisms. UPS or XPS spectra are calculated by the GW approximation (GWA), which well reproduces the energy gap and band structures. This year, we have mainly focused on the program tuning of TOMBO using fortran90, MPI and openMP on the system B (SGI) and the system C (FX10) of ISSP. As an application of TOMBO, we have calculated the band structure of  $\text{TiO}_2$  and  $\text{ZnO}$  by using the GWA [1,2]. For example, Fig. 1 represents the resulting band structure of rutile  $\text{TiO}_2$  with Nb impurities ( $\text{Ti}_{0.75}\text{Nb}_{0.25}\text{O}_2$ ) [1]. Dots and curves represent the GWA and the LDA results, respectively, and energy zero is set at the top of the valence band. There is an occupied impurity level in the middle of the band gap and an empty impurity level just below the conduction band. The result well agrees with the

experiment [3].

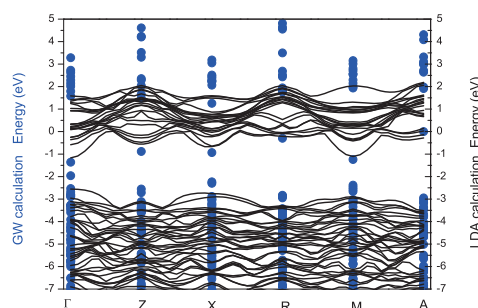


Fig.1 GW band structure of  $\text{Ti}_{0.75}\text{Nb}_{0.25}\text{O}_2$  [1].

In this year, we opened source code of LDA part as well as WINDOWS executable of the TOMBO program from our home page [4,5].

## References

- [1] M. Zhang, S. Ono, and K. Ohno, *Phys. Rev. B* **92**, 035205 (2015).
- [2] M. Zhang, S. Ono, N. Nagatsuka, and K. Ohno, *Phys. Rev. B* **93**, 155116 (2016).
- [3] D. Morris, Y. Dou, J. Rebane, C. E. J. Mitchell, R. G. Egdell, D. S. L. Law, A. Vittadini, and M. Casarin, *Phys. Rev. B* **61**, 13445 (2000).
- [4] S. Ono, Y. Noguchi, R. Sahara, Y. Kawazoe, and K. Ohno, *Comp. Phys. Comm.* **189**, 20-30 (2015).
- [5] <http://www.ohno.ynu.ac.jp/tombo/index.html>

# Computational-Science Study of Frustrated Magnets

Hiroki NAKANO

*Graduate School of Material Science, University of Hyogo  
3-2-1 Kouto, Kamigori-cho, Ako-gun, Hyogo 678-1297, Japan*

It is well known that to study quantum spin systems is generally difficult because they are typical many-body problems. For such studies, therefore, computational approaches become more important. Each method among the computational ones, however, has not only merits but also demerits. Quantum Monte Carlo method faces with a so-called negative sign problem when a system includes frustrations in it although this method can treat large systems if they do not include frustrations. Density matrix renormalization group (DMRG) method can treat frustrated systems. This method, however, is powerful to a one-dimensional system; the extension of this method to systems in dimensions larger than one is now developing. Numerical-diagonalization method, on the other hand, is a reliable way irrespect of the point whether or not a target system is frustrated and irrespect of spational shape of the system. The most serious weak point of this method is that this method can treat only very small systems. To overcome this weak point, we developed an MPI-parallelized code of numerical diagonalizations based on the Lanczos algorithm[1]. This code can treat systems with its sizes that are larger than those determined by computer resources when calculations are carried out in a single node.

The primary study of the present project is to clarify the behavior of the magnetization process of the spin- $S$  Heisenberg anti-ferromagnet on the kagome lattice by means of the Lanczos-diagonalization code mentioned in the above[2]. The magnetization process for the  $S = 1/2$  case has been extensively studied[3, 4, 5, 6]; however, there are few studies for the cases of larger  $S$ . For  $S = 1$ , the magnetization process was reported in Ref. 3.

When  $S$  is large, the increase of the dimension of the Hamiltonian matrix for the increase of the system sizes becomes more rapid. Therefore, the weak point of the numerical-diagonalization method becomes more serious; there are no reports for  $S > 1$  to the best of our knowledge. Under circumstances, we clarify the behavior of the magnetization processes for various spin- $S$  cases from  $S = 1$  up to  $S = 5/2$ . We successfully observed the existence of the magnetization plateau at one-third of the height of the saturation in the magnetization process. The existence is irrespect of  $S$ . We discuss the  $S$  dependences of the edge fields and the width of the plateau and find a significant difference between our numerical-diagonalization results and results obtained by real-space perturbation theory[7].

Our result of a quantum spin system by large-scale parallelized calculations of Lanczos diagonalization make the true behavior of the system. Our large-scale Lanczos-diagonalization study contributes much to our understandings of these systems.

## References

- [1] H. Nakano and A. Terai: J. Phys. Soc. Jpn. **78**, 014003 (2009).
- [2] H. Nakano and T. Sakai: J. Phys. Soc. Jpn. **84** (2015) 063705.
- [3] K. Hida: J. Phys. Soc. Jpn. **70** (2001) 3673.
- [4] H. Nakano and T. Sakai: J. Phys. Soc. Jpn. **79** (2010) 053707.
- [5] T. Sakai and H. Nakano: Phys. Rev. B **83** (2011) 100405(R).



- [6] H. Nakano and T. Sakai: J. Phys. Soc. Jpn. **83** (2014) 104710.
- [7] M. E. Zhitomirsky: J. Phys.: Conf. Ser. **592** (2015) 012110.

# Ordering of topological excitations of the frustrated magnets

Tsuyoshi OKUBO

*Institute for Solid State Physics, University of Tokyo  
Kashiwa-no-ha, Kashiwa, Chiba 277-8581*

Frustrated spin systems have attracted much recent interest because of their novel orderings. In two-dimensional frustrated Heisenberg spin systems, a topologically stable point defect, a  $Z_2$  vortex, often plays an important role. A possible topological phase transition driven by binding-unbinding of the  $Z_2$  vortices was proposed by Kawamura and Miyashita about 30 years ago [1]. In this  $Z_2$  vortex transition, the spin correlation length keeps finite. At the  $Z_2$ -vortex transition temperature  $T = T_v$ , only the vortex correlation length characterizing the typical separation of the free vortices diverges. This is a sharp contrast to the case of the Kosterlitz-Thouless transition in two dimensional  $XY$  spin systems, where the spin correlation length diverges together with the vortex correlation length below the transition temperature.

The nature of the possible  $Z_2$ -vortex transition has been investigated typically on the triangular-lattice Heisenberg antiferromagnet. Recent Monte Carlo simulation up to  $L = 1536$  suggested the occurrence of  $Z_2$ -vortex transition at a finite temperature  $T_v/J \simeq 0.285$  with a finite spin-correlation length  $\xi \simeq 2000$  [2]. However, the existence of topological phase transition has not been fully resolved because the observed spin correlation length is larger than the maximum system size. In order to clarify the true nature of the  $Z_2$ -vortex transition, we need larger systems beyond the spin-correlation length at the transition temperature.

In order to perform such larger scale Monte Carlo simulations, we consider an effective model of two-dimensional frustrated Heisenberg magnets. The Hamiltonian of the model is given by

$$\mathcal{H} = -\frac{J}{4} \sum_{\langle i,j \rangle} \text{Tr} R_i R_j^t \quad (J > 0), \quad (1)$$

where  $R_i$  is a  $SO(3)$  rotation matrix on the site  $i$ , and  $\sum_{\langle i,j \rangle}$  means the sum over the nearest-neighbor pairs on the square lattice. This effective model does not have explicit frustrated interactions. However, it has topological  $Z_2$  vortices, and therefore we expect the  $Z_2$ -vortex binding-unbinding transition at a finite temperature as similar to the frustrated Heisenberg spin systems. For the Monte Carlo simulation of this unfrustrated model, we can use Wolff-Swendsen-Wang type cluster algorithm, which is not efficient for the frustrated interactions. We have implemented MPI parallelized cluster algorithm for this model and investigated nature of possible  $Z_2$ -vortex transition by extensive Monte Carlo simulation of the model. The lattice is a  $L \times L$  square lattice with periodic boundary conditions.

In this year project, we performed Monte Carlo simulation for  $L \leq 16384$  on the ISSP system B and the kei computer. In order to investigate the  $Z_2$ -vortex transition, we consider the free-energy cost against vortex formation,  $\Delta V(L)$ . The free-energy cost is expected to be proportional to the logarithm of the system

size  $L$  as

$$\Delta V(L) \sim C + v \log L, \quad (2)$$

where the coefficient  $v$  is called ‘‘vorticity modulus’’. The vorticity modulus is an order parameter of the  $Z_2$  vortex transition: it takes a finite value for  $T < T_v$ , while  $v = 0$  for  $T > T_v$ . In Fig.1, we show the temperature dependence of the vorticity modulus calculated from two sizes ( $L_1, L_2 = L_1/2$ ) as

$$v(L_1, L_2) \equiv \frac{\Delta V(L_1) - \Delta V(L_2)}{\log L_1/L_2}. \quad (3)$$

We see that the vorticity modulus increases around  $T/J \simeq 0.28$ , indicating a finite-temperature phase transition. We define the effective transition temperature as the temperature where vorticity modulus across  $v = 0$ . A preliminary extrapolation assuming the existence of  $Z_2$ -vortex transition leads  $T_v/J \simeq 0.27$ , which is considered as the upper bound of  $T_v$ . On the other hand, the spin correlation length at this temperature is estimated at least  $\xi \simeq 20000$  lattice spacings. Because the present system is limited  $L \leq 16384$ , which is comparable with the correlation length at the estimated  $T_v$ , we need a careful analysis to conclude the existence of the finite-temperature topological phase transition.

## References

- [1] H. Kawamura and S. Miyashita: J. Phys. Soc. Jpn. **53** (1984) 4138.
- [2] H. Kawamura, A. Yamamoto, and T. Okubo: J. Phys. Soc. Jpn. **79** (2010) 023701.

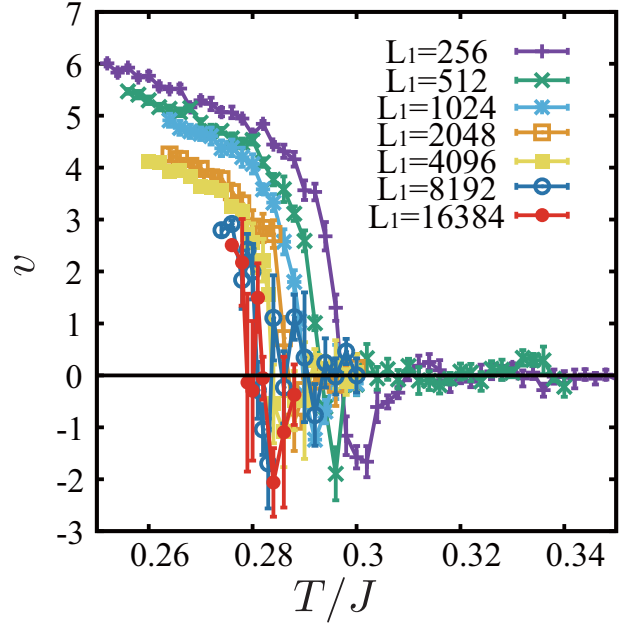


Figure 1: Vorticity modulus as a function of the temperature for various systems sizes  $128 \leq L \leq 16384$ .

# Large-scale computational simulations of non-equilibrium transport phenomena

Yoshihiro ASAI, Marius BÜRKLE, Jun-ichi OZAKI

*Research Center for Computational Design of Advanced Functional Materials National Institute of Advanced Industrial Science and Technology (AIST),  
Central 2, Umezono 1-1-1, Tsukuba, Ibaraki 305-8568*

We have studied the following subjects in the context of non-equilibrium transport in terms of large-scale computational simulations:

- 1) The effect of short-range strong correlation on the electric conductance and the electric current at finite bias voltage.
- 2) Electric conductance and electric current calculations based on an order-N DFT method for large channel materials.
- 3) Phonon transport calculation based on the first-principles DFT theory.
- 4) Thermopower calculation for materials in the hopping transport regime.
- 5) Phonon effects on the electric current noise including shot noise and temperature noise.
- 6) First-principles non-equilibrium Green's function (NEGF) calculations of the I-V characteristics of non-volatile memory materials.
- 7) Comparisons of first-principles transport calculations with scanning tunneling microscope break junction experiments.

In the following we outline these subjects and give the main:

- 1) Calculations were made in terms of the time dependent DMRG method. The Hubbard chain model was adopted for the channel. Firstly, we focused our attention to the length dependence of the conductance and found a damped oscillatory behavior, which indicates the inelastic contribution from the strong onsite repulsion  $U$  on the conductance. **【submitted to PRL: 1】**
- 2) The non-equilibrium Green's function (NEGF) method based transport code was combined with the CONQUEST code for order-N calculation of large systems. It was tested for some hundred nm length channel materials for the conductance. Finite voltage calculation code has been also implemented. **【unpublished: 2】**
- 3) Phonon transport calculations without and with phonon-phonon scattering were made for two terminal devices with a single molecule as a channel material. **【PRB: 3, unpublished: 4】**

- 4) The Seebeck coefficient was calculated in terms of the self-consistent theory of electron and phonon currents (PRB 78, 045434 (2008)) using the extended Su-Schrieffer-Heeger model. The result was used to discuss the base alignment dependence of the Seebeck coefficient for DNA. **【Nature Commun.: 5】**
- 5) The phonon transport and the electronphonon coupling effects on the electric current noise including shot noise and temperature noise was discussed using a full counting statistics approach. **【PRB, Rapid Commun.: 6】**
- 6) The I-V characteristic and the material dependence of the ON/OFF ratio of the current were investigated using the first-principles NEGF transport calculation results on the resistive random access memory cells **【PCCP: 7 and 8】** and the interfacial phase change memory cells **【unpublished: 9】**. A lowest order expansion method was used to discuss the phonon effect in the former case.
- 7) Our first-principles NEGF calculation results were compared with scanning tunneling microscope (STM) break junction experiments showing fair agreement with each other.

## References

- [1] J. Ozaki and Y. Asai, submitted to Phys. Rev. Lett.
- [2] Unpublished.
- [3] M. Bürkle, T.J. Hellmuth, F. Pauly, and Y. Asai: Phys. Rev. B, **91**, 165419 (2015).
- [4] Unpublished.
- [5] Y. Li, Limin X. J. L. Palma, Y. Asai and N. J. Tao: Nature Communications, **7**, 11294-1-8 (2016).
- [6] Y. Asai: Phys. Rev. B, **91**, 161402 (R) (2015).
- [7] H. Nakamura and Y. Asai: Phys. Chem. Chem. Phys. **18**, 8820 (2016).
- [8] X. Zhong, I. Rungger, P. Zapol, H. Nakamura, Y. Asai and O. Heinonen: Phys. Chem. Chem. Phys. **18**, 7502 (2016).
- [9] Unpublished.
- [10] S. -K. Lee, M. Buerkle, R. Yamada, Y. Asai and H. Tada, Nanoscale, **7**, 20497 (2015).
- [11] D. Miguel, L.Á. de Cienfuegos, A. Martín-Lasanta, S.P. Morcillo, L.A. Zotti, E. Leary, M. Bürkle, Y. Asai, R. Jurado, D.J. Cárdenas, G. Rubio-Bollinger, N. Agraït, J.M. Cuerva, and M.T. González: J. Am. Chem. Soc. **137**, 13818 (2015).
- [12] R. García, M.Á. Herranz, E. Leary, M.T. González, G. Rubio-Bollinger, M. Bürkle, L.A. Zotti, Y. Asai, F. Pauly, J. C. Cuevas, N. Agraït and N. Martín, Beilstein: J. Org. Chem. **11**, 1068 (2015).